

6. 名古屋大学医学部附属病院外科病棟 における DVT 予防の実際

名古屋大学医学部附属病院看護部 横山 恵
名古屋大学医学部血管外科 錦見尚道

1) 予防ガイドラインの作成および実施方法

当院では、2002（平成14）年にDVT、肺血栓塞栓症（PTEまたはPE）を予防するためのガイドラインを医療安全管理室と血管外科医師を中心にして独自に作成した。これは、①簡便にハイリスク患者をスクリーニングすること、②適切な対策方法を誰でも容易に選択できることを特徴としている。主には、①DVT/PE要因票（表1）を用いて重症度を点数化することと、②その点数に基づきDVT/PE予防方法（表2）に準じ対策を選択することの2段階で実施できる。

具体的には、まずDVT/PE要因票に基づき、治療要因と身体要因の2つの側面を点数化する。この合計が3点以上の場合、向血栓性素因のスクリーニングを中心とした血液凝固検査を追加し異常がないかを確認する¹⁾。さらに追加検査で血液凝固系の機能に異常を認めた場合は、すでに深部静脈血栓が存在していないかをカラードプラで確認し、異常があった場合は血管外科医師にコンサルトして対応策を講じる（表1）。

予防方法は点数にしたがって段階的に設定されており、高得点つまりハイリスク患者には弾性ストッキングや間欠的空気圧迫装置（intermittent pneumatic compression：IPC）の使用および低分子ヘパリン（非分画ヘパリンも可）の投与を勧めている。リスクに応じて複数の対策方法が設定してあり、その患者に対して実行可能な方法を選択することができる（表2）。

IPCはハイリスク患者が多い外科病棟やICUに配置されており、使用することになった患者では、病棟から手術室に持ち込み、手術中から使用している。

2) 手術前後のDVT/PE予防の実際

手術を受けることが決定したら、担当医師は外来でDVT/PE要因票に基づきリスクの程度を確認する。当院の外科で行われている手術はほとんどが予定時間

263-00215

表1 DVT/PE要因票 2003年2月版

治療要因	
1. 60歳以上かつ予定時間1時間以上の全身麻酔手術	2点
2. 40歳以上かつ予定時間3時間以上の全身麻酔手術	2点
3. 60歳以上で気腹を用いる手術	1点
4. 術後に下肢の運動を制限する必要がある（経大腿動脈動脈造影・血管内治療を含む）	1点
5. 術後などに水分制限下の安静を必要とする	1点
治療要因計 点 (A)	
身体要因	
1. 過去に、深部静脈血栓症・肺塞栓症を起こした事がある	5点
2. 血縁者に、深部静脈血栓症・肺塞栓症を起こした人がいる	3点
3. 過去に、急に膝から下が腫れて痛くなった事がある	4点
4. 血縁者に、急に膝から下が腫れて痛くなった事がある人がいる	3点
5. 凝固制御因子の異常を指摘されたことがある	5点
6. 3回以上連続して流産を繰り返したことがある	3点
7. 1日の大半をベッド上で過ごす	1点
8. あまり水分を取らない/取らないように指示されている	1点
9. 妊娠している/経口避妊薬内服中である	1点
10. 1年以上ステロイドを内服している	1点
身体要因計 点 (B)	
A+B= 点	
A+Bが3点以上の場合には、血液凝固追加検査	
異常の場合	
ア. ATⅢ、Protein C、Protein S 活性値の測定（註：肝機能や経口抗凝固薬の影響を受ける）	5点
イ. D-Dimer（高値、かつ動脈瘤・左房内血栓など動脈内血栓性疾患がない場合）	5点
ウ. 抗β ₂ GPI抗体	5点
エ. 抗CL抗体（PT正常範囲でかつAPTTが正常値以下の低下認められた場合）	5点
註：アからエの検査は、結果が出るまでに○日間かかります。	
血液凝固追加検査に異常を認めた時	
下肢静脈還流検査カラードップラによる形態学的検査または静脈還流機能検査を行う	
異常の場合、血管外科受診で個別対応します。	還流は正常の場合
最終合計点 点	
処置予定日 20__年__月__日	
記入医師名：	記入看護師名：

表2 DVT/PE予防方法 2003年2月版

手術患者		チェックリスト
5点以上	GEC+IPC（病院備品）を継続的に使用する	<input type="checkbox"/> GEC購入
	術式により可能ならばLMWH投与を勧める	<input type="checkbox"/> IPCの使用申込
	この場合、LMWH適応外使用のインフォームド・コンセントを得ておく	◎ LMWH承諾 ◎ LMWH非承諾
	同意が得られなければLMWHは使用しない	<input type="checkbox"/> LMWH在庫確認
	LMWHの投与、持続点滴或いは皮下注で、歩行開始後3日後まで続ける	
	IPCの使用期間は術後2日か、歩行開始まで続ける	
	GECは退院まで装着し、退院後1ヶ月の装着を勧める	
4点	GEC+IPC（病院備品）	<input type="checkbox"/> GEC購入
	IPCは術中から術後1日、術後2日目から歩行開始までは用手マッサージ等	<input type="checkbox"/> IPCの使用申込
	GECは退院まで装着し、退院後1ヶ月の装着を勧める	
2～3点	GECを歩行開始まで使用	<input type="checkbox"/> GEC購入
	以後は、臥床時下肢挙上	
0～1点	適切な輸液、早期離床	
経大腿動静脈処置患者		チェックリスト
4点以上	GEC+用手マッサージ/足関節運動	<input type="checkbox"/> GEC購入
	GECは退院まで装着し、退院後1ヶ月の装着を勧める	
2～3点	GECを歩行開始まで使用	<input type="checkbox"/> GEC購入
	以後は、臥床時下肢挙上	
0～1点	適切な輸液、早期離床	
GEC：弾性ストッキング（足関節部圧迫圧20mmHg）		購入先
IPC：間欠的空気圧迫装置（AV-impulse、フロートロンなど）		使用申込先
LMWH：低分子ヘパリン75IU/kg/day		申請先

3時間以上の全身麻酔手術であり、手術後は1日の大半をベッド上で過ごすことになり、3点以上となる。このため手術を受ける患者のほぼ全例が弾性ストッキングを使用している。

患者への説明は、まず医師から手術の説明を行うと同時に合併症としてDVTが発症する可能性があること、その予防対策として弾性ストッキングを着用する必要があることを説明する。その後、看護師から体位変換・ベッド上での下肢の運動・早期離床など、手術後にストッキング着用とともに行うDVTを予防する

方法を説明する。

予防に用いる場合のストッキングは、男性でも一人で着用することが簡便なハイソックスタイプを使用している。患者の下腿周囲径を測定して、適切なサイズを選択している。

手術当日は出棟前に弾性ストッキングを着用して手術室へ入室する。帰棟後は体位変換とともに、臥床中の下肢の運動を促している。できるだけ早期に離床を進め、初回の歩行はストッキングを着用したままで、看護師が介助して行う。

その後、さらに離床を進め、トイレ歩行が自由に行えるようになるまではストッキングを着用している。乳房や甲状腺の手術のように手術翌日に自由に歩行が可能となる場合は術後2日目まで、開腹手術の場合は術後3日目から10日目ぐらまではストッキングを着用している。

ハイリスクでIPCの使用が必要な患者も同様にストッキングを着用している。ベッド上で過ごす期間は6時間おきに30分間の空気圧迫をストッキングの上から行っている。ガイドラインでは1カ月程度のストッキングの着用を勧めているため、できるだけ長期間着用するように指導している。

IPCは4点以上の場合だけでなく、肥満体型で主治医から使用を指示される場合や生体部分肝臓移植手術のドナーに使用している。

ガイドラインの運用当初はストッキングを自費購入していた。しかし、2004（平成16）年4月から肺血栓塞栓症予防管理料として会計請求できるようになり、病院側から医療材料としてストッキングを準備しているため、予防対策が必要な場合は全員がストッキングを着用できている。

おわりに

2003（平成15）年2月から7月までに集積した457例の評価票で、凝固制御因子欠乏症（プロテインC or S）が5例以上あり、4例ではDVTの既往がなく、さらに2例では65歳以上の高齢者であった²⁾。モンゴロイドにはFactor V Leidenの報告がないことはよく知られているが、凝固制御因子欠乏症の有病率は意外と多いのかもしれない。

当院で行っているDVT/PE予防法がどれだけ有効であるかは、このガイドラインの試行前後の発症率を比較しなければ不明である。残念なことに、病院全体

ではガイドライン試行前のデータを得ることは困難である。また、現在提示している治療要因・患者要因の点数づけの有効性に関しては、今後詳細な解析を行う必要がある。

■ 文献

- 1) 錦見尚道, 上田裕一, 高松純樹: 向血栓性素因のスクリーニング検査. 静脈学, 14: 315-318, 2003.
- 2) 錦見尚道: 高齢者手術の安全性の向上および術後合併症の予防に関する研究 (H14-長寿-015)・平成15年度総括分担研究報告書. 2004年3月, p.21-22.
- 3) 肺塞栓症/深部静脈血栓症 (静脈血栓塞栓症) 予防ガイドライン作成委員会: 肺塞栓症/深部静脈血栓症 (静脈血栓塞栓症) 予防ガイドライン—ダイジェスト版—2004, メディカルフロントインターナショナル, 東京, 2004.



Regulation of mouse GADD34 gene transcription after DNA damaging agent methylmethane sulfonate

Masataka Haneda^{a,b}, Hengyi Xiao^a, Tadao Hasegawa^a, Yuko Kimura^a,
Izumi Nakashima^b, Ken-ichi Isobe^{a,*}

^aDepartment of Basic Gerontology, National Institute for Longevity Sciences, 36-3 Gengo, Morioka-cho, Obu, Aichi 474-8522, Japan

^bDepartment of Immunology, Nagoya University School of Medicine, 65 Turumai-cho, Showa, Nagoya, Aichi 466-8520, Japan

Received 19 December 2003; received in revised form 23 March 2004; accepted 13 April 2004

Available online 7 June 2004

Received by R. Di Lauro

Abstract

The GADD34 gene is transcriptionally induced by growth arrest and DNA damage. However, the mechanisms underlying the transcriptional regulation are still unclear. We analyzed the promoter of mouse GADD34 gene and the methylmethane sulfonate (MMS)-induced transcriptional regulation of this gene. By introducing genome mutants, which were linked to the luciferase reporter, into NIH3T3 cells, we defined a 100-bp fragment upstream of the transcriptional initiating site as the minimal promoter of the GADD34 gene. Subsequent study revealed that CRE-binding site located in this minimal promoter was critical for MMS-induced transcription of the GADD34 gene. In vitro binding experiments showed that phosphorylated c-Jun was contained in the CRE/DNA complex. Overexpression of the dominant negative form of c-Jun led to a decrease of MMS-responsive promoter activity. From these results, we conclude that the CRE site of the GADD34 promoter is indispensable to the MMS-responsive *cis*-element that c-Jun is the essential transcription factor for MMS-stimulated regulation of GADD34 gene expression and that the upstream signaling is dependent on JNK.

© 2004 Elsevier B.V. All rights reserved.

Keywords: GADD34; Transcription; DNA damage; Stress response; c-Jun

1. Introduction

In mammalian cells, the response to genotoxic stress enhances DNA repair, transient growth arrest, and/or apoptosis. The 5 GADD genes, GADD7, GADD33, GADD34, GADD 45, and GADD153, were originally isolated after ultraviolet irradiation in Chinese hamster ovary (CHO) cells (Fornace et al., 1989). The GADD34 gene is the human/hamster homologue of the mouse MyD116 cDNA that was subsequently isolated as a primary response transcript expressed during myeloid differentiation of mouse M1 myeloid leukemia cells (Abdollahi et al., 1991). Moreover, GADD genes have a growth-inhibitory function and one or

a combination of these GADD genes suppress cell growth (Zhan et al., 1994). The GADD34 protein has a region of homology with the herpes simplex virus-1 (HSV-1) protein 134.5 (Chou and Roizman, 1994; He et al., 1996). The carboxyl-terminal domain of gamma 134.5 has the structural and functional attributes of a subunit of protein phosphatase 1 (PP1) specific for eukaryotic translation initiation factor 2 alpha (eIF2 α), which it has evolved to preclude shut-off of protein synthesis. Recently, other groups (Novoa et al., 2001, 2003) and we (Kojima et al., 2003) have reported one function of GADD34 under endoplasmic reticulum (ER) stress. ER stress induces the GADD34 gene expression. GADD34 binds to PP1 and this complex specifically dephosphorylates eIF2 α , which precludes the shut-off of new protein synthesis.

Because GADD34 was originally cloned after genotoxic stresses, GADD34 appears to possess another function that relates to genotoxic stresses. We have shown that transfection of GADD34 enhances the phosphorylation of p53 at

Abbreviations: GADD, growth arrest and DNA damage; MMS, methylmethane sulfonate.

* Corresponding author. Tel.: +81-562-44-5651; fax: +81-562-44-6591.

E-mail address: kenisobe@nils.go.jp (K. Isobe).

Ser15, and induces p21/WAF1 transcription via the p53 binding site (Yagi et al., 2003). Further, we have found that GADD34 is engaged in the pathway, which suppresses cell growth by genotoxic stress (unpublished data). The next step to determine how GADD34 is regulated by genotoxic stresses. Here, we cloned mouse GADD34 genome and determined DNA sequence of GADD34. We analyzed the GADD34 transcription induced by genotoxic stress, MMS. We defined the MMS-responsive *cis*-element and transcription factors that induce GADD34 promoter activity.

2. Materials and methods

2.1. Cell culture and reagents

NIH3T3 cells from the American type culture collection (ATCC, Rockville, MD) were maintained in a 37 °C humidified atmosphere containing 5% CO₂ with Dulbecco's modified Eagle's medium (Sigma) supplemented with 10% fetal calf serum (GIBCO). Methylmethane sulfonate (MMS) was purchased from Sigma-Aldrich (St. Louis, MO).

2.2. Genome library

We subcloned the lambda FIX II genome library (Stratagene) using the mouse GADD34 probe designed the –250- to +40-bp range (+1 was the relative start site of the GADD34 promoter) and amplified it by polymerase chain reaction (PCR) using the mouse genome as a template. The PCR amplified fragment was subcloned into a TA cloning vector (Promega) and sequences were confirmed by dideoxy sequencing. Restriction fragment mapping and preliminary DNA sequencing of various subclones revealed the organization of the mouse GADD34 gene.

2.3. Plasmid constructs

GADD34 promoter-containing reporters were constructed as follows. pGL3b –4.0 kbp was constructed via insertion of a 4.0-kbp fragment of the mouse GADD34 promoter region, from –4.0 kbp to +100 bp relative to the TATA box, into a firefly luciferase reporter vector, pGL3-basic, at BglII sites. The GADD34 5'-deletion constructs were all based on the promoter-less luciferase reporter gene vector pGL3basic. A series of scanning mutants between GADD34 –100 and +49 bp were prepared by PCR amplification using the mouse genome as a template, employing different mutated 5'-oligonucleotide primers and a 3'-primer. The oligonucleotides used in these mutagenesis reactions were as follows: pGL3b-0.2 kbp, 5'-TACGTGAGATCGACGGCTCT-3' and 5'-CAGCGC-GCCCTATAGCGTAC-3'; pGL3b-55bp, 5'-CCTTTTCCCAGGGACTTCCG-3' and 5'-CAGCGCGCCCTATAGCGTAC-3'; pGL3b-CRE, 5'-CGA-GTCTCGACCTCTCCGGT-3' and 5'-CAGCGCGCCCTATAGCGTAC-3'; and pGL3-TATA, 5'-

CTCCGGTGACAACAGCACAGCC-3' and 5'-CAGCGCGCCCTATAGCGTAC-3'. The fragments were subcloned into TA cloning vectors (Promega) and mutant sequences were confirmed by dideoxy sequencing. pCRE-luc, pAP1-luc and pTAL-luc vectors were purchased from Clontech. The pTAL-luc contains the firefly luciferase (*luc*) gene fused to a TATA-like (TAL) promoter region from the Herpes simplex virus thymidine kinase (HSV-TK) promoter. The pCRE-luc contains the firefly luciferase gene and has five copies of the CRE-binding sequence fused to the pTAL-luc vector. The pAP1-luc contains the firefly luciferase gene and has five copies of the AP1-binding sequence. The mammalian expression vectors employed in this study were driven by the cytomegalovirus (CMV) promoter. Dominant-negative c-Jun (TAM67) and dominant-negative ATF-2 (ATF2-dn) expression vectors were a kind gift from Dr. Xiao. The dominant-negative CREB (kcreb)expressions vector was purchased from Clontech.

2.4. Transient transfection and reporter gene assay

NIH3T3 cells were planted onto 24-well plates at a density of 20,000 cells/well. Cells were transfected with 100 ng/well of plasmids by the effectene transfection reagent (Clontech). MMS treatment was started 24 h after transfection, and several hours later cells were lysed and luciferase assays in the lysates were measured by luminometer. The transfection efficiency was estimated via cotransfection with thymidine kinase promoter-driven Renilla luciferase reporter vector (pRL-TK plasmid, dual luciferase assay system, Promega).

2.5. Electrophoretic mobility shift assays

Nuclear extracts from either proliferating or MMS-treated NIH3T3 cells were prepared as described (Hasegawa et al., 1999). A total of 5 µg of the nuclear extract was incubated with 5 fmol of ³²P end-labeled double-strand oligonucleotides with a sequence corresponding to the region from –31 to –14 bp from TATA box in the GADD34 promoter. Incubation was carried out in 1 volume of 10 µl at room temperature for 20 min. All binding reactions contained 10 mM Tris-HCl (pH 7.5), 4% glycerol, 50 mM NaCl, 0.5 mM EDTA, 0.5 mM dithiothreitol (DTT), 1 mM MgCl₂, and 0.5 mg/ml of poly (di-dC). For competition, 1 pmol of unlabeled oligonucleotides were incubated in the reaction. In supershift experiments, 1 µl of antibody was added 10 min before the labeled probe. The electrophoretic mobility shift assay (EMSA) products were separated on a 4% polyacrylamide 0.5 × Tris-borate EDTA gel at room temperature at 150 V for 90 min. The gel was dried and subjected to autoradiography. The oligonucleotides used in these experiments were as follows: CRE-probe: 5'-TCCGGTGACGTCAGCACAGCCC-3' and mutated CRE-probe: 5'-TCCGGTGACAACAGCACAGCCC-3'. The antibodies directed against c-Jun, ATF-2 and CREB and phosphorylated c-Jun, ATF-2 and CREB antibodies were

purchased from Cell Signaling Biotech: anti-c-Jun antibody (#9126), anti-phospho-c-Jun antibody (#9164), anti-ATF-2 antibody (#9222), anti-phospho-ATF-2 antibody (#9221), anti-CREB antibody (#9192), and anti-phospho-CREB antibody (#9191). Anti-mouse IgG antibody was purchased from Amersham.

2.6. Immunoblotting

Total cell lysates from either proliferating or MMS-treated NIH3T3 cells were prepared as described (Xiao et al., 1999). Cells were washed with ice-cold phosphate-buffered saline (PBS) twice and lysed with an ice-cold lysis buffer containing 10 mM HEPES (pH 7.4), 30 mM NaCl, 2% glycerol, 0.2% NP-40, 0.3 mM MgCl₂, 0.2 mM EDTA, 1 mM phenylmethylsulfonyl fluoride (PMSF), 1 mg/ml leupeptine. Cytoplasmic extracts and nuclear extracts were prepared as previously described. Twenty-five micrograms of lysates was electrophoresed on 8%, 10%, or 12% SDS-polyacrylamide gels. Proteins were detected using a chemiluminescent ECL kit (Amersham) with one of the following antibodies: anti-c-Jun antibody (#9126), anti-phospho-c-Jun (Ser63) antibody (#9164), anti-phospho-ATF-2 (Thr71) antibody (#9221), anti-phospho-CREB (Ser133) antibody (#9191), anti-phospho-p38 antibody (Thr180/Tyr182) (#9211), anti-phospho-SEK1(Thr223) (#9151, Cell Signaling Technology) or anti-GADD34 antibody (C-19, Santa Cruz).

2.7. Statistics

Geometric means are expressed with S.E.M. Statistical significance of the differences among various groups was evaluated by two-way repeated-measures ANOVA. Differences were considered to be significant when $p < 0.01$.

3. Results

3.1. Organization of the mouse GADD34 gene

Using the mouse GADD34 probe, two positive clones, lambda FIX II 13 and 26, were identified. Restriction fragment mapping and DNA sequencing of various subclones revealed the organization of the mouse GADD34 gene (Fig. 1). The exon–intron organization of the mouse GADD34 gene was determined by direct DNA sequencing using oligodeoxynucleotide primers. A given exon–intron boundary was indicated when the sequence from genomic clones diverged from that of the cDNA. The entire mouse

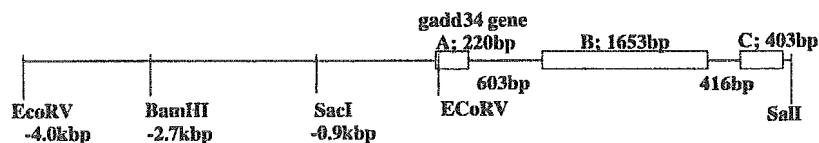


Fig. 1. Structure of the mouse GADD34 gene. Exon are indicated by boxes and designated as A, B and C. Restriction sites are shown.

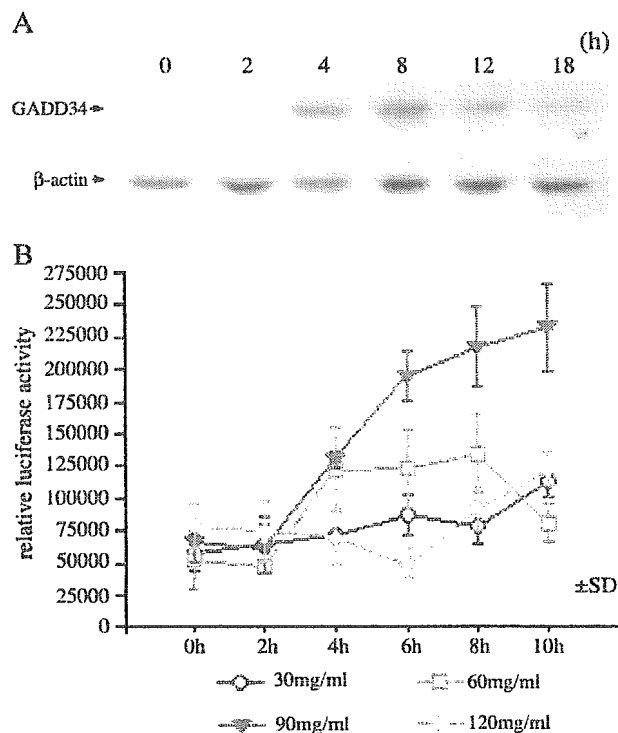


Fig. 2. Induction of GADD34 gene after MMS treatment. (A) Total cell lysates from either non-treated or MMS-treated NIH3T3 cells were obtained at appropriate time points (at 0, 2, 4, 8, 12 and 18 h). Proteins were detected by chemiluminescent ECL kit (Amersham). (B) Influence of MMS on the transcriptional activity of the mouse GADD34 promoter 4.0-kbp luciferase-reporter construct in NIH3T3 fibroblasts. NIH3T3 cells were transiently transfected with mouse GADD34 promoter 4.0 kbp (pGL3b-4.0 kbp) and stimulated with MMS (0, 30, 60, 90, 120 μ g/ml) for various time periods. Results were correlated with renilla luciferase activity that came from co-transfected pRL-TK, and expressed as relative luciferase activity. The results were the mean of four transfections from two separate experiments. The error bars indicate the S.E.M.

GADD34 gene comprises three exons. The 900-bp-promoter region of the mouse GADD34 gene was completely sequenced from both strands. DNA sequences surrounding the mouse GADD34 gene transcriptional start site are highly GC-rich and have a TATA box.

3.2. Induction of mouse GADD34 promoter activity by MMS

MMS treatment invoked GADD34 expression at 4 h after MMS treatment. Activity peaked at 8 h and continued to 18 h (Fig. 2A). We investigated GADD34 promoter

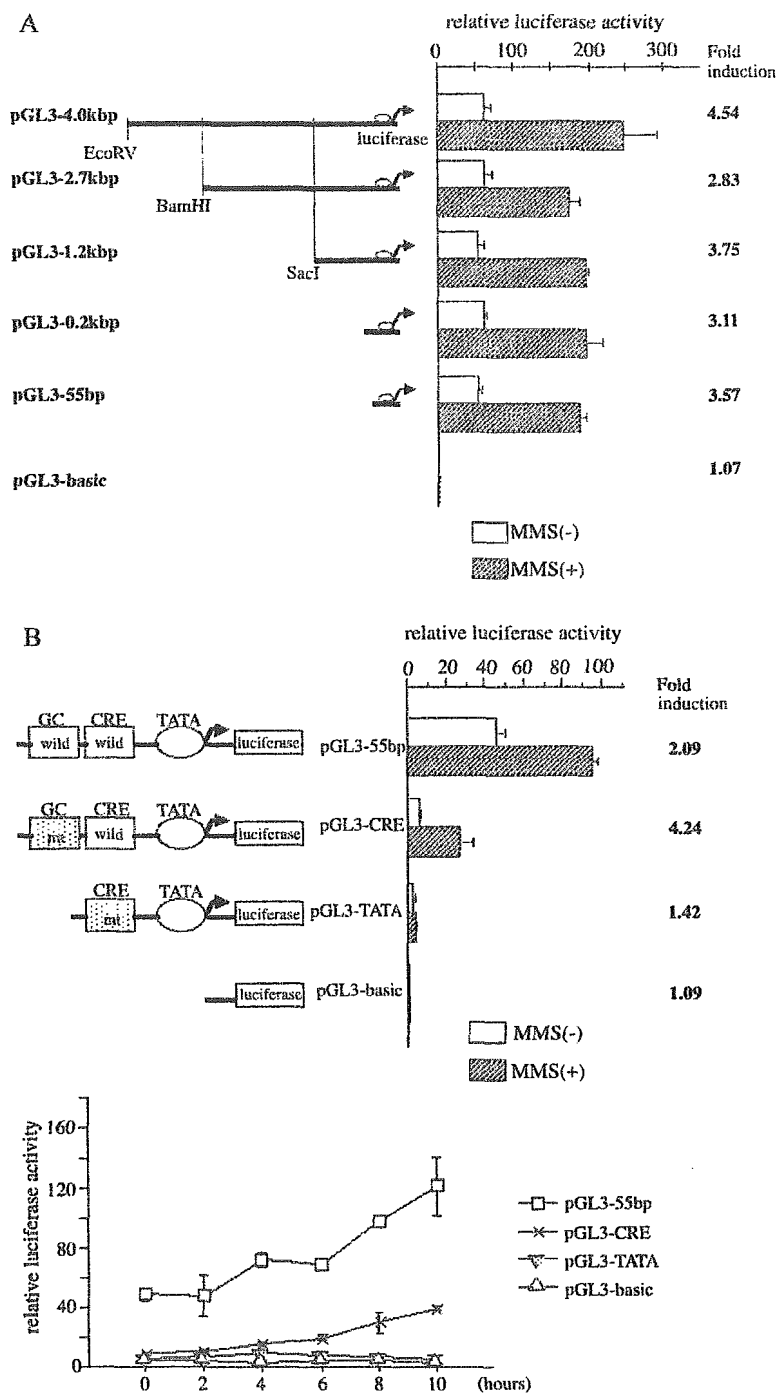


Fig. 3. Analysis of GADD34 5'-deletion mutants and mutagenesis of the mouse GADD34 core promoter in NIH3T3 cells. (A) NIH3T3 cells were transiently transfected with mouse GADD34 5'-deletion mutants of different length and incubated with or without MMS (90 μ g/ml) for 8 h. Cell lysates were subsequently analyzed for luciferase activity. (B) The pGL3-55bp, pGL3-CRE, pGL3-TATA and pGL3-basic reporter constructs were transiently transfected into NIH3T3 cells. MMS stimulation and luciferase assay were performed as above. (C) Analysis of the transcriptional activity of the CRE consensus promoter vector (pCRE-luc) in MMS-treated NIH3T3 fibroblasts. NIH3T3 cells were transiently transfected with pCRE-luc, AP1-luc and pTAL-luc vectors and incubated with or without MMS (90 μ g/ml) for 12 h. Cell lysates were subsequently analyzed for luciferase activity. The results were the mean of four transfections from two separate experiments. The error bars indicate the S.E.M.

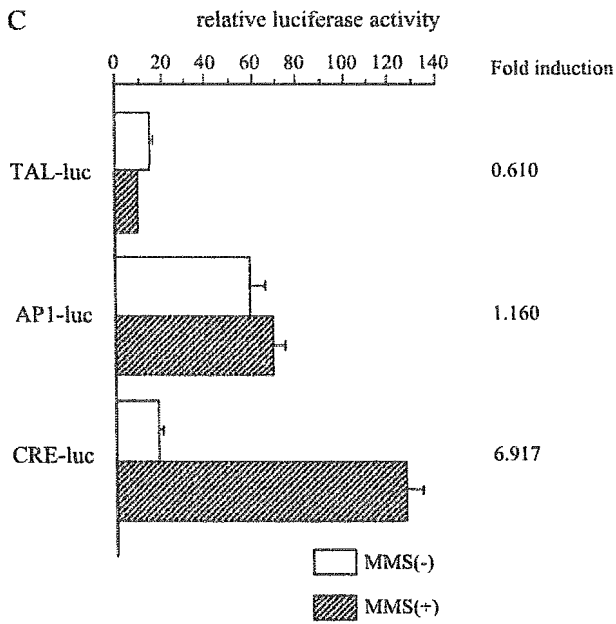


Fig. 3 (continued).

activity using the cells transiently transfected with pGL3b-4.0 kbp, driven by our longest mouse GADD34 promoter in the luciferase reporter gene. As shown in Fig. 2B, GADD34 promoter activity increased immediately and peaked at 10 h after incubation with a dose of 90 µg/ml MMS. Lysates from the cells transfected with pGL3b-4.0 kbp showed a 2.5-fold induction following treatment of 90 µg/ml MMS relative to the basal activity of this construct in untreated cells. A dose response was observed: increasing dose resulted in increasing promoter activity and the higher dose of MMS treatment delayed the maximal response. Because 120 µg/ml MMS resulted in 20% survival, we performed the following experiment with a dose of 90 µg/ml MMS.

3.3. Mapping of basal core promoter and MMS-responsive element in mouse GADD34 promoter

To elucidate the MMS-responsive regions of the mouse GADD34 promoter, NIH3T3 cells were transfected transiently with a series of 5' terminus-truncated mutants of the GADD34 promoter linked to the luciferase reporter gene.

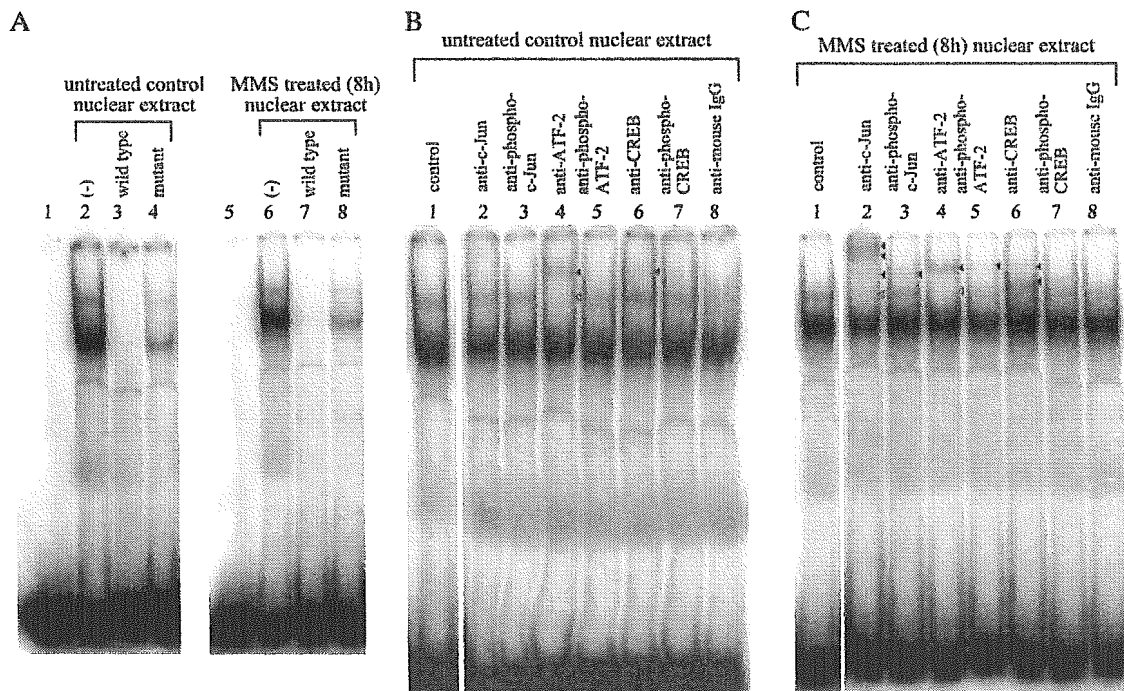


Fig. 4. EMSA of the mouse GADD34 – 31 to – 14 bp region. For EMSA experiments, double-strand oligonucleotides were synthesized and ³²P-end labeled. (A) Double-strand labeled probes were incubated with untreated NIH3T3 cell nuclear extracts (lanes 2 to 4) or MMS-treated nuclear extract (lanes 6 to 8), and in the presence of unlabeled (cold) consensus oligonucleotides (lanes 3 and 7) and mutant oligonucleotides (lanes 4 and 8). Lanes 1 and 5 were without nuclear extract. (B) For supershift assays, untreated NIH3T3 nuclear extracts were pre-incubated with antibodies prior to addition of the probe. Lane 1: without antibody, lane 2: with anti-c-Jun antibody, lane 3: with anti-phospho-c-Jun antibody, lane 4: with anti-ATF-2 antibody, lane 5: with anti-phospho-ATF-2 antibody, lane 6: with anti-CREB antibody, lane 7: with anti-phospho-CREB antibody, and lane 8: with anti-mouse IgG antibody. Solid triangle bar shows supershift complexes and open triangle bar shows diminished complexes. (C) MMS-treated NIH3T3 nuclear extracts were pre-incubated with antibodies prior addition of the probe. Lanes 1 to 8 numbering is same as (B).

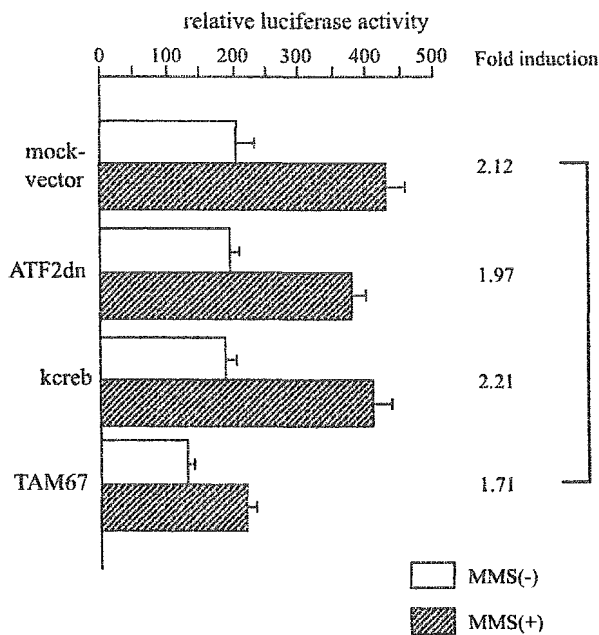


Fig. 5. Influence of dominant negative forms of c-Jun on GADD34 promoter activity in MMS-treated NIH3T3. Cells were transiently cotransfected with TAM67, ATF-2dn and kcreb expression vectors and pGL3-55 bp, and incubated with or without MMS (90 μ g/ml) for 12 h. Cell lysates were subsequently analyzed for luciferase activity. The results were the mean of four transfections from two separate experiments. The error bars indicate the S.E.M. *Significantly different from control ($p < 0.01$).

As shown in Fig. 3A, the basal activities of the mutant promoters remained at the same level until truncation up to -55 bp (100-bp fragment, from -55 to -40 bp relative to TATA box; pGL3b-55 bp, 100 bp upstream of GADD34 initiation start site). The basal activity of constructs shorter than -55 bp dramatically decreased. 5'-Deletion analysis of GADD34 5'-flanking DNA revealed that -55 bp upstream of the GADD34 TATA box is able to confer full responsiveness to MMS. According to database analysis (TFSEARCH: Searching Transcription Factor Binding Sites (ver 1.3) Web site: <http://www.cbrc.jp/research/db/TFSEARCH.html>), we noticed that there are consensus protein binding elements in this region. A DNA-stretch spanning -42 to -33 bp is comprises putative binding sites for GC-box, and the region between -27 and -20 bp represented a consensus CRE/CREB element. A mutation in the GC-box site decreased basal transcription (Fig. 3B). These results suggest that the GC-box and the CRE located in the minimal promoter are the basal transcription element of the GADD34 promoter. On the other hand, a mutation in the CRE site decreased MMS-induced transcription. These results suggest that the CRE site located in the minimal promoter is the *cis*-responsive element for MMS-induced transcription of the GADD34 promoter.

To investigate whether the CRE site is the MMS-responsive element, either the pCRE-luc vector or pAP1-luc vector

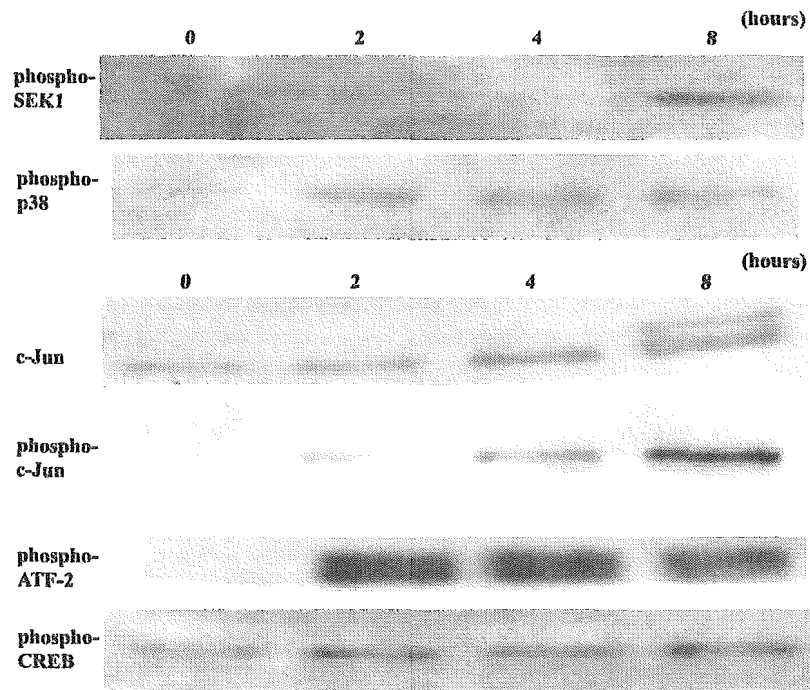


Fig. 6. MMS-treatment induced SEK1 activation and c-Jun phosphorylation. Total cell lysates from either non-treated or MMS-treated NIH3T3 cells were obtained at appropriate time points (at 0, 2, 4 and 8 h). Proteins were detected by chemiluminescent ECL kit (Amersham).

was transfected into NIH3T3 cells (Fig. 3C). Lysates from the cells transfected with pCRE-luc had a 6.9-fold induction of luciferase activity by the MMS treatment relative to the basal activity of this construct in untreated cells. Conversely, lysates from the cells transfected with pAPI-luc had only a 1.2-fold induction.

3.4. *c-Jun* binding to the CRE site increased by MMS treatment, while ATF-2 nor CREB did not

As the sequence of CRE of GADD34 promoter was identical to the consensus sequence of CRE/CREB, we investigated by EMSA assay whether the complexes consisted of *c-Jun*, ATF-2 or CREB. The addition of *c-Jun* (lane 2), ATF-2 (lane 4) or CREB (lane 6) antibody to the binding reaction caused the complexes to be supershifted (Fig. 4A). By the MMS treatment, the amount of *c-Jun* or phospho-*c-Jun* supershift increased (Fig. 4B). Conversely, the amount of ATF-2, phospho-ATF-2, CREB or phospho-CREB supershift was not obviously changed by the MMS treatment.

3.5. Overexpression of dominant negative forms of *c-Jun* repressed GADD34 promoter activity by MMS treatment

In order to confirm the EMSA assay, we used the dominant negative form of *c-Jun*, CREB or ATF-2. When the dominant negative form of *c-Jun* (TAM67) expression constructs was co-transfected with pGL3b-55bp into NIH3T3 cells, reporter gene activity was repressed after MMS treatment (Fig. 5). However, neither dominant negative forms of ATF-2 (ATF2-dn) nor CREB (kcreb) overexpression had any effect on MMS-induced transcriptional activity.

3.6. Upstream signaling of MMS-responsive GADD34 promoter activity

ATF-2 was phosphorylated at 2 h after MMS treatment, and continued to 8 h. Both protein amount of *c-Jun* and that of phospho-*c-Jun* (ser67) increased from 2 h and maximized at 8 h. SEK1, which phosphorylates *c-JUN* NH₂-terminal kinase 1/2 (JNK1/2) and activates JNK, was phosphorylated at 8 h after MMS treatment (Fig. 6).

4. Discussion

This is the first report to analyze mouse GADD34 promoter activity. Using 5' promoter deletion analysis, we have shown that the minimal basal activity of GADD34 is about –55 bp from the TATA box. By site directed mutagenesis, we concluded that the CRE site is indispensable to the MMS-responsive *cis*-element. Both the GC-box and the CRE site are also found in tandem upstream of the TATA box of human and hamster GADD34 genes (Hollander et al., 1997). By EMSA analysis we have shown that *c-Jun*, ATF-2 and CREB

specifically bound the GADD34 promoter element. Although three factors bind to the CRE site of the GADD34 promoter (Fig. 4A), only *c-Jun* and phospho-*c-Jun* increase the binding to the GADD34 CRE site at –27 to –20 bp by MMS treatment. The transcription factor *c-Jun* is one component of AP-1 that binds and activates transcription at AP1 sites. UV irradiation and growth factors stimulate phosphorylation of *c-Jun* and activate *c-Jun*-dependent transcription (Derijard et al., 1994; Kyriakis et al., 1994). As *c-Jun* gene expression depends on transcription factor *c-fos*, a specific inhibitor of MEK1 might decrease the expression of *c-fos*, but PD 98059 did not influence MMS-induced luciferase activity of the GADD34 promoter (data not shown). As consensus reporter vectors showed that the CRE site is more responsive than the AP-1 site, we concluded that CRE site is essential for MMS-stimulate regulation of the GADD34 promoter.

Here we analyzed transcription of the GADD34 gene by genotoxic stress. Recent findings show that GADD34 works under both ER stress (Novoa et al., 2001, 2003; Kojima et al., 2003) and DNA damaging stress (Yagi et al., 2003 and our unpublished data). Transcriptional regulation of GADD34 induced by both ER stresses and genotoxic stresses is important. ATF3 has been recently shown to work as a transcription factor for the ER stress-induced GADD34 promoter by using the same CRE binding site (Jiang et al., 2004). ER stress inducer thapsigargin activates PERK, which phosphorylates eIF2 α . The phosphorylated eIF2 α stops new protein synthesis and induces GADD34 gene expression. GADD34 dephosphorylates eIF2 α and recovers from protein synthesis arrest. The question then becomes whether or not MMS treatment induces ER stresses. However, we found that MMS did not stimulate eIF2 α phosphorylation or induce the shut-off of new protein synthesis (unpublished data). GADD34 was transcriptionally expressed by the MMS treatment, which induces DNA damaging stress but not ER stress. Here, we concentrated on the transcription of GADD34 induced by genotoxic stress. GADD153, which is also induced by genotoxic stresses, uses the C/EBP-ATF composite site for transcription. The regulation of GADD153 gene transcription induced by arsenite was up-regulated by ATF-4 and repressed by ATF-3 (Fawcett et al., 1999).

Monofunctional alkylating agents like MMS are potent inducer of cellular stresses that lead to chromosomal aberrations and point mutations. Also such alkylating agents are ubiquitous in our environment, and are also produced endogenously by cells as natural metabolites. MMS has been shown to induce mitogen activation protein kinases (MAPKs) (Wilhelm et al., 1997). MAPKs comprise a ubiquitous family of tyrosine/threonine kinase and include extracellular signal-regulated kinase (ERKs), *c-JUN* NH₂-terminal kinase (JNKs) and p38MAPKs. Although some studies have revealed a relation between GADD45 or GADD153 and MAPKs, the relation between GADD34 and MAPKs has not yet been elucidated. Here we have shown that JNK is one of the upstream signals of GADD34 gene transcription.

References

- Abdollahi, A., Lord, K.A., Hoffman-Liebermann, B., Liebermann, D.A., 1991. Interferon regulatory factor 1 is a myeloid differentiation primary response gene induced by interleukin 6 and leukemia inhibitory factor: role in growth inhibition. *Cell Growth Differ.* 2, 401–407.
- Chou, J., Roizman, B., 1994. Herpes simplex virus 1 gamma(1)34.5 gene function, which blocks the host response to infection, maps in the homologous domain of the genes expressed during growth arrest and DNA damage. *Proc. Natl. Acad. Sci. U. S. A.* 91, 5247–5251.
- Derijard, B., Hibi, M., Wu, I.H., Barrett, T., Su, B., Deng, T., Karin, M., Davis, R.J., 1994. JNK1: a protein kinase stimulated by UV light and Ha-Ras that binds and phosphorylates the c-Jun activation domain. *Cell* 76, 1025–1037.
- Fawcett, T.W., Martindale, J.L., Guyton, K.Z., Hai, T., Holbrook, N.J., 1999. Complexes containing activating transcription factor (ATF)/cAMP-responsive-element-binding protein (CREB) interact with the CCAAT/enhancer-binding protein (C/EBP)-ATF composite site to regulate Gadd153 expression during the stress response. *Biochem. J.* 339, 135–141.
- Fornace Jr., A.J., Nebert, D.W., Hollander, M.C., Luetthy, J.D., Papathanasiou, M., Fargnoli, J., Holbrook, N.J., 1989. Mammalian genes coordinately regulated by growth arrest signals and DNA-damaging agents. *Mol. Cell. Biol.* 9, 4196–4203.
- Hasegawa, T., Xiao, H., Isobe, K., 1999. Cloning of a GADD34-like gene that interacts with the zinc-finger transcription factor which binds to the p21(WAF) promoter. *Biochem. Biophys. Res. Commun.* 256, 249–254.
- He, B., Chou, J., Liebermann, D.A., Hoffman, B., Roizman, B., 1996. The carboxyl terminus of the murine MyD116 gene substitutes for the corresponding domain of the gamma(1)34.5 gene of herpes simplex virus to preclude the premature shutoff of total protein synthesis in infected human cells. *J. Virol.* 70, 84–90.
- Hollander, M.C., Zhan, Q., Bae, I., Fornace Jr., A.J., 1997. Mammalian, 1997. GADD34, an apoptosis- and DNA damage-inducible gene. *J. Biol. Chem.* 272, 13731–13737.
- Jiang, H.Y., Wek, S.A., McGrath, B.C., Lu, D., Hai, T., Harding, H.P., Wang, X., Ron, D., Cavener, D.R., Wek, R.C., 2004. Activating transcription factor 3 is integral to the eukaryotic initiation factor 2 kinase stress response. *Mol. Cell. Biol.* 24, 1365–1377.
- Kojima, E., Takeuchi, A., Haneda, M., Yagi, A., Hasegawa, T., Yamaki, K., Takeda, K., Akira, S., Shimokata, K., Isobe, K., 2003. The function of GADD34 is a recovery from a shutoff of protein synthesis induced by ER stress: elucidation by GADD34-deficient mice. *FASEB J.* 17, 1573–1575.
- Kyriakis, J.M., Banerjee, P., Nikolakaki, E., Dai, T., Rubie, E.A., Ahmad, M.F., Avruch, J., Woodgett, J.R., 1994. The stress-activated protein kinase subfamily of c-Jun kinases. *Nature* 369, 156–160.
- Novoa, I., Zeng, H., Harding, H.P., Ron, D., 2001. Feedback inhibition of the unfolded protein response by GADD34-mediated dephosphorylation of eIF2alpha. *J. Cell Biol.* 153, 1011–1022.
- Novoa, I., Zhang, Y., Zeng, H., Jungreis, R., Harding, H.P., Ron, D., 2003. Stress-induced gene expression requires programmed recovery from translational repression. *EMBO J.* 22, 1180–1187.
- Wilhelm, D., Bender, K., Knobel, A., Angel, P., 1997. The level of intracellular glutathione is a key regulator for the induction of stress-activated signal transduction pathways including Jun N-terminal protein kinases and p38 kinase by alkylating agents. *Mol. Cell. Biol.* 17, 4792–4800.
- Xiao, H., Hasegawa, T., Isobe, K., 1999. Both Sp1 and Sp3 are responsible for p21waf1 promoter activity induced by histone deacetylase inhibitor in NIH3T3 cells. *J. Cell. Biochem.* 73, 291–302.
- Yagi, A., Hasegawa, Y., Xiao, H., Haneda, M., Kojima, E., Nishikimi, A., Hasegawa, T., Shimokata, K., Isobe, K., 2003. GADD34 induces p53 phosphorylation and p21/WAF1 transcription. *J. Cell. Biochem.* 90, 1242–1249.
- Zhan, Q., Lord, K.A., Alamo Jr., I., Hollander, M.C., Carrier, F., Ron, D., Kohn, K.W., Hoffman, B., Liebermann, D.A., Fornace Jr., A.J. 1994. The gadd and MyD genes define a novel set of mammalian genes encoding acidic proteins that synergistically suppress cell growth. *Mol. Cell. Biol.* 14, 2361–2371.

Protein phosphatase 1, but not protein phosphatase 2A, dephosphorylates DNA-damaging stress-induced phospho-serine 15 of p53

Masataka Haneda^{a,b}, Eiji Kojima^a, Akihiko Nishikimi^a, Tadao Hasegawa^a, Izumi Nakashima^b, Ken-ichi Isobe^{a,*}

^aDepartment of Basic Gerontology, National Institute for Longevity Sciences, 36-3 Gengo, Morioka-cho, Obu, Aichi 474-8522, Japan

^bDepartment of Immunology, Nagoya University School of Medicine, 65 Turumai-cho, Showa-ku, Nagoya, Aichi 466-8520, Japan

Received 7 January 2004; revised 11 April 2004; accepted 14 April 2004

Available online 8 May 2004

Edited by Varda Rotter

Abstract Okadaic acid (OA) is a protein phosphatase (PP) inhibitor and induces hyperphosphorylation of p53. We investigated whether the inhibition of PP1 by OA promotes the phosphorylation of the serine 15 of p53. *In vitro* dephosphorylation assay showed that PP1 dephosphorylated ultraviolet C (UVC)-induced phospho-ser15 of p53, and that OA treatment inhibited it. One of the PP1 regulators, growth arrest and DNA damage 34 (GADD34), disturbed PP1 binding with p53, interfered with the dephosphorylation of p53 and increased the amount of phospho-p53 after UVC-treatment. This report provides the first evidence that PP1, but not PP2A, dephosphorylates phospho-serine 15 of p53.

© 2004 Federation of European Biochemical Societies. Published by Elsevier B.V. All rights reserved.

Keywords: Okadaic acid; DNA-damaging stress; p53 Phosphorylation; Protein phosphatase 1; Protein phosphatase 2A; GADD34

1. Introduction

Tumor suppressor p53 is tightly regulated by phosphorylation. The phosphorylated p53 induces cell-growth arrest and/or apoptosis through p53 response gene transcription. DNA-damaging stress, such as γ -irradiation and ultraviolet (UV) irradiation, activates ATM/ATR kinases, which in turn phosphorylate the serine 15 residue of p53 protein [1]. The phosphorylated serine 15 promotes the interaction with p300 [2], and p300 acetylated p53 and histones, which enhances promoter activity of p53 response gene. It remains unclear whether phospho-serine 15 stabilizes p53 protein. On the other hand, the serine 20 residue of p53 is phosphorylated by CHK proteins [3–5], and is the important site of interaction to MDM2 protein. Phosphorylation of serine 20 dissociates from MDM2, which promotes p53 stability [6].

It has been shown that multiple protein phosphatases (PPs) can dephosphorylate p53 *in vitro*. These phosphatases include

PP1, PP2A, PP5, Wip1 and Cdc14 [7–10]. Under normal condition, PP1/PP2A dephosphorylates the C-terminal of p53 protein; this site is phosphorylated by protein kinase C, which influences the DNA binding ability of p53 and transcriptional activity [11]. Meanwhile, the phosphorylation at the N-terminal of p53 is important for transcription and stabilization [12,13], but dephosphorylation of that site has not been well studied. Okadaic acid (OA), the inhibitor of PP1 and PP2A [14], accumulates hyperphosphorylated p53 [15,16] and the PP2A inhibitor, SV40 small t antigen, promotes the DNA binding ability of p53 and the transcriptional activity [17]. One of the PP1 regulators, growth arrest and DNA damage 34 (GADD34) (PPP1R15A, myd116), increases the amount of total and phosphorylated p53, and promotes p21 (waf1) mRNA expression [18]. These studies show that PPs regulate p53 through these phosphatase activities. Under stressed condition, however, the relations between PPs and p53 have been unclear.

In the present study, we show the relation between p53 and PP1 under DNA damaging conditions. We demonstrate that OA increases the amount of phosphorylation at the serine 15, which is related to the inactivation of PP1. Furthermore, by using GADD34 deficient MEFs, we show that the regulation of PP1 influenced p53 phosphorylation *in vivo*. These results suggest that PP1 is the key regulator of p53 and is the major phosphatase of phospho-serine 15 of p53.

2. Materials and methods

2.1. Cell lines and transfection

Human WI38 cells and HEK293 cells were maintained in Dulbecco's modified Eagle's medium (GIBCO) supplemented with 10% fetal bovine serum (GIBCO). Human p53 null cell lines SOAS-2 were maintained in modified McCoy's 5A medium (GIBCO) with 15% fetal bovine serum (FBS). All cells were grown at 37 °C in a humidified atmosphere of 5% CO₂. Transfections were performed with the effectene reagent (Qiagen). Methyl methanesulfonate (MMS) was purchased from Sigma–Aldrich.

2.2. Preparation of mouse embryonic fibroblasts

Mouse embryonic fibroblasts (MEFs) from GADD34-deficient mice and wild-type mice were prepared from 14.5-day-old embryo [19]. All cultures were maintained in Dulbecco's modified essential medium (Sigma) with 10% FBS. Cells were plated 2 × 10⁶ cells/10-cm plates for subculture.

* Corresponding author. Fax: +81-562-44-6591.
E-mail address: kenisobe@nils.go.jp (K.-i. Isobe).

Abbreviations: OA, okadaic acid; GADD, growth arrest and DNA damage; UVC, ultraviolet C; MMS, methyl methanesulfonate

2.3. Plasmids

Human p53 expression vector was provided by Bai and Merchant [20]. PPI cDNA was purchased from Invitrogen and cloned into the *Bam*HI/*Xba*I site of pcDNA3.1HisA vector with Xpress tag. Mouse GADD34 myc-tagged expression vector was described previously [18]. SV40 small t antigen cDNA was obtained by polymerase chain reaction (PCR) amplification using the cDNA of COS-1 cells as a template and employing 5'- and 3'-oligonucleotide primers. The oligonucleotides used in this experiment were as follows: small t antigen 5'-probe: 5'-CGGGATCCATGGATAAAGTTTTAAACAGAG-3'; small t antigen 3'-probe: 5'-CCGCTCGAGTTAGAGCTTTAAATCTCTGTA-3'. The fragments were subcloned into the *Bam*HI/*Xba*I site of pcDNA3.1HisA vectors. Sequences were confirmed by dideoxy sequencing. When cDNA expression vectors were transfected, protein synthesis was inhibited by the phosphorylation of eukaryotic translation initiation factor 2 alpha (eIF2 α). We employed pAdVantage vector (Promega) to preclude the termination of protein synthesis.

2.4. DNA-damaging and phosphatase-inhibitor treatments

WI38 cells and MEFs were grown to 50–80% confluence in 6-cm dishes in DMEM containing 10% FBS. DNA damage was achieved by exposing the cells to ultraviolet C (UVC) (50 J/m²) or MMS (80 μ g/ml). Cells were harvested at indicated time points. In some experiments, they were treated with increasing concentrations of OA (from 1 to 100 nM) 6 h before DNA-damage treatment. Four hours after irradiation, cells were treated with 10 μ g/ml of cyclohexamide to arrest new p53 protein synthesis and cells were then harvested at the indicated time points. OA and cyclohexamide were purchased from Sigma.

2.5. Immunoblotting

Proteins were analyzed by SDS-PAGE and detected by a chemiluminescent ECL kit (Amersham) with one of the following antibodies: anti-p53 antibody, anti-phospho-ser15 p53 antibody (Cell signaling), anti-GFP antibody (BD Biosciences), anti-GADD34 antibody (Santa Cruz), anti-eIF2 α antibody (Santa Cruz), anti-phospho-ser 51 eIF2 α antibody (BIOSOURCE international), anti-p21 (waf1) antibody (Santa Cruz), and anti- β -actin antibody (Amersham).

2.6. In vitro dephosphorylation assay

WI38 cells were UVC-treated (100 J/m²) and 1 h later the cells were lysed in low-stringency buffer (50 mM Tris-HCl, pH 7.5; 120 mM NaCl; 0.5 mM EDTA; and 0.5% NP-40) in the presence of PMSF and protease inhibitors. After pre-cleaning with protein G beads (Amersham), the extracts were immunoprecipitated with anti-p53 antibody in the presence of protein G beads for 4 h at 4 °C. The beads were then washed three times with low-stringency buffer, and twice with PPI reaction buffer containing 1 mM MnCl₂ and 5 mM caffeine. One unit of PPI (New England Biolabs, Inc.) was added to the immune complexes for 1 h at 30 °C. For inhibition studies, the immune complexes and PPI were incubated with 1 μ M of OA in PPI reaction buffer for 1 h at 30 °C. For positive control studies, Calf intestine alkaline phosphatase (CIAP) (Takara) was added to the immune complexes in CIAP buffer for 1 h at 37 °C. Dephosphorylation was analyzed by SDS-PAGE and was detected by immunoblotting with anti phospho-serine 15 of p53 antibody.

3. Results

3.1. Okadaic acid increases UVC-induced phosphorylation at serine 15 residue of p53

OA is an inhibitor of PPI and PP2A. To evaluate the role of PPI/PP2A in regulating p53 phosphorylation after DNA-damaging stress, WI38 cells were exposed to UVC (50 J/m²) with increasing concentrations of OA. As shown in Fig. 1, the high concentrations of OA (100 nM) induced an increase in phosphorylated serine 15 of p53. On the other hand, the low concentrations of OA (1 nM) slightly reduced the phosphorylation of p53 after UVC treatment. The same treatment did not affect the amount of β -actin. These results demonstrate

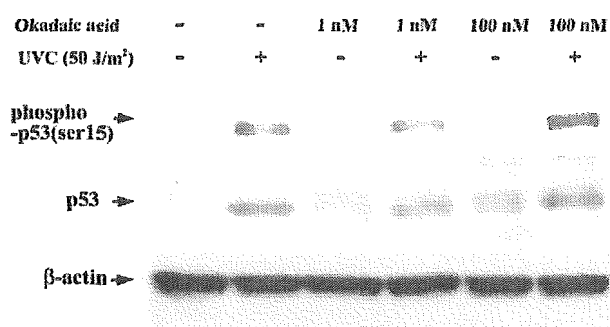


Fig. 1. OA increases p53 phosphorylation by UVC treatment. WI38 cells were treated by UVC (50 J/m²) for 4 h with increasing concentrations of OA. Phosphorylated p53 (top panel) and total p53 (middle panel) were determined. As a control, β -actin levels were determined (bottom panel). These are the representative data of more than two experiments.

that PPI and/or PP2A regulated the phosphorylation at the serine 15 of p53 through phosphatase activity.

3.2. Protein phosphatase 1, but not protein phosphatase 2A, is the key regulator of phospho-serine 15 of p53

High concentrations of OA (100 nM) promoted the phosphorylation of p53, but it was unclear whether PPI or PP2A was more important for the regulation of phospho-serine 15 of p53. To rule out the possibility that PP2A dephosphorylates p53, the PP2A inhibitor, SV40 small t antigen, was co-transfected to the culture cells to block p53 dephosphorylation. After UVC treatment, small t antigen did not affect the amount of p53, but induced a decrease in phospho-serine 15 of p53 (Fig. 2). To confirm the possibility that PPI dephosphorylates p53, the PPI regulator protein, GADD34, was co-transfected to the cultured cells to block p53 dephosphorylation. After UVC treatment, mouse GADD34 increased the amount of p53 and induced phosphorylation at the serine 15 of p53 (Fig. 2). These results suggested that GADD34 interfered in the dephosphorylation of p53, causing an increase in phospho-serine 15.

3.3. Protein phosphatase 1 dephosphorylates the serine 15 residue of p53 in vitro

Because we found that PPI bound p53 in vivo, we next investigated whether PPI could actually dephosphorylate phospho-ser15 of p53. We employed in vitro dephosphorylation assay. As shown in Fig. 3, PPI dephosphorylated UVC-induced phospho-ser15 of p53. 1 μ M of OA treatment inhibited the phosphatase activity of PPI. CIAP also dephosphated p53.

3.4. The PPI regulator GADD34 enhances DNA damage-induced p53 phosphorylation

To determine the relation between p53 phosphorylation and GADD34, we analyzed the p53 protein expression and p53 phosphorylation using GADD34 deficient MEFs. In wild-type MEFs, GADD34 was induced 8 h after MMS treatment (Fig. 4). And the protein levels of p53 and phospho-serine 18 of mouse p53 (corresponding to serine 15 of human p53) were highly expressed in a time-dependent manner at 8 h after MMS treatment. On the other hand, in GADD34-deficient MEFs, the levels of both p53 and phospho-serine 18 of p53

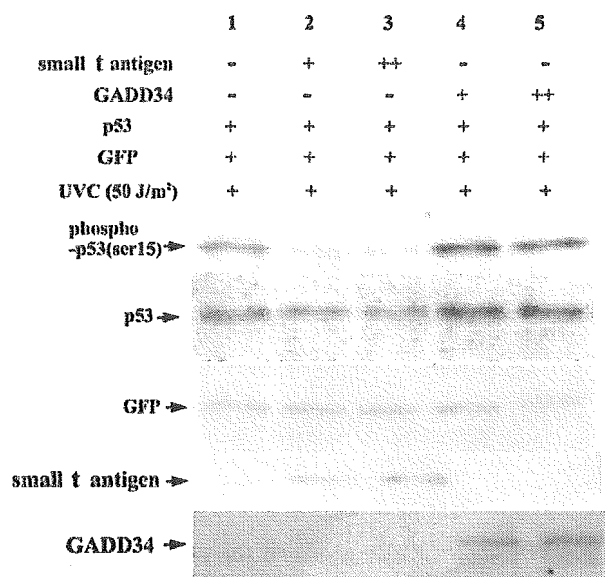


Fig. 2. Mouse GADD34 promotes phospho-ser 15 of p53 and interferes with the interaction between PP1 and p53. GADD34 promotes phosphorylation of p53 at serine 15, but SV40 small t antigen decreases phospho-serine 15. SOAS-2 cells were transfected with 0.1 μ g of human p53 wild-type, 0.1 μ g of GFP and 0.2 μ g of Advantage vector (all lanes), and co-transfected with one or more of the following vectors: 0.2 μ g of mock vector (lane 1), 0.1 μ g of mock vector and 0.1 μ g of small t antigen expression vector (lane 2), 0.2 μ g of small t antigen expression vector (lane 3), 0.1 μ g of mock vector and 0.1 μ g of mouse GADD34 expression vector (lane 4), and 0.2 μ g of GADD34 expression vector (lane 5). Phospho-ser 15 of p53 (top panel) and total p53 (middle panel) were determined. GFP was determined as the transfection internal control (bottom panel). These are the representative data of more than two experiments.

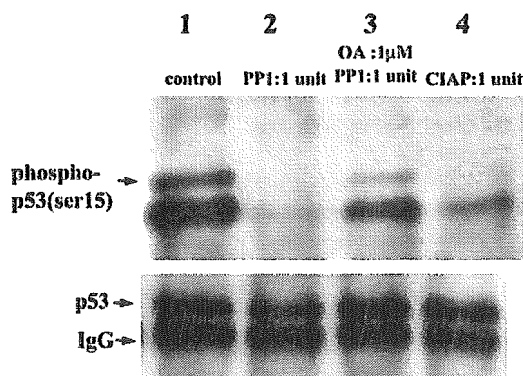


Fig. 3. PP1 dephosphorylates phospho-ser15 of p53 in vitro. WI38 cells were UVC-treated (100 J/m²) and p53 protein was immunoprecipitated with anti-p53 antibody. As a control, the immune complexes were incubated without PP1 (lane 1). One unit of PP1 was added to the complexes (lane 2). For inhibition studies, the complexes and PP1 were incubated with 1 μ M of OA (lane 3). As a positive control, CIAP was added to the complexes (lane 4). The products were probed with anti phospho-serine 15 of p53 antibody (upper panel). Same membrane was re-probed with anti p53 antibody (lower panel). These are the representative data of more than two experiments.

expressions were lower than in wild-type MEFs. The fold induction of phosphorylated p53 per total p53 by MMS treatment was lower than that of wild-type MEFs. In GADD34-deficient MEFs, the level of p21 (waf1, cip1) expression was

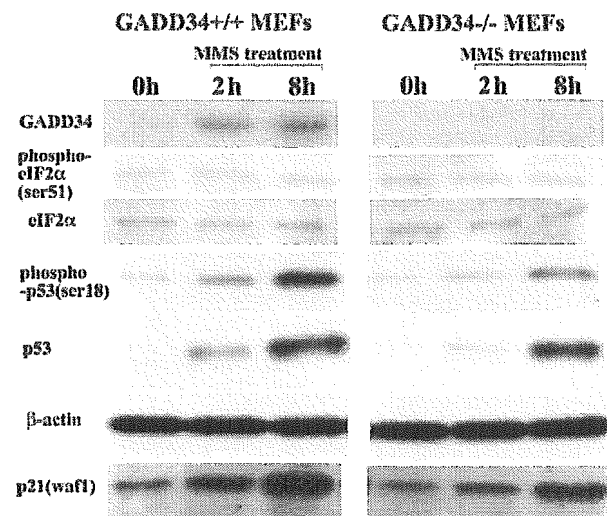


Fig. 4. Determination of p53 and phospho-p53 protein levels in wild-type and GADD34 deficient MEFs after MMS treatment. Cells were treated with 80 μ g/ml MMS and cell lysates were prepared at the indicated time points. 50- μ g lysate was run on 10% SDS-PAGE. To investigate the status of protein synthesis, we examined total eIF2 α and phosphorylated eIF2 α . Total p53, phosphorylated p53 and p21 (waf1) were determined by immunoblotting. As a control, β -actin levels were determined. These are the representative data of more than two experiments.

lower than that in wild-type MEFs. MMS treatment, unlike endoplasmic reticulum (ER) stress, did not induce the phosphorylation of eIF2 α (Fig. 4). The same treatment did not affect the expression of β -actin, indicating that GADD34 protein did not have an overall positive effect on protein expression after MMS treatment.

4. Discussion

PP1 is the cellular protein serine/threonine phosphatase and the regulator of protein function through dephosphorylation. Here, we showed that OA treatment enhanced the phosphorylation of p53 at serine 15 after UVC treatment (Fig. 1). OA is the inhibitor of PP1 and PP2A, and this agent inhibits PP2A (50% inhibitory dose IC₅₀, 1–10 nM) more potently than PP1 (IC₅₀, 100 nM to 1 μ M) [21]. Since 100 nM OA promoted the phosphorylation of p53, PP1 was thought to be more important in phospho-serine 15 of p53. To rule out the possibility that PP2A dephosphorylates p53, the PP2A inhibitor, SV40 small t antigen, was co-transfected with p53 expression vector to block p53 dephosphorylation. After UVC treatment, small t antigen did not affect the amount of p53, but induced a decrease in phospho-serine 15 of p53 (Fig. 2). The corresponding mechanisms remain unknown, but it is suggested that PP2A may act as a negative regulator of PP1 or activate the serine 15 kinase.

The PP1 regulator, GADD34 (PPP1R15A, myd116), is induced by ER stress [19,22,23], and GADD34 relocates PP1 to ER for dephosphorylation of eIF2 α . We employed GADD34 to confirm the possibility that PP1 dephosphorylates p53. After UVC treatment, co-transfected mouse GADD34 expression increased the amounts of total and phospho-ser 15 of

p53 (Fig. 2). By using GADD34 deficient MEFs, we confirmed the relation between GADD34 and p53 phosphorylation (Fig. 4). In a previous study, we reported that PP1 regulator GADD34 induced phospho-serine 15 of p53 and promoted p21 (waf1) mRNA expression through p53 DNA binding sites [18].

The phosphorylation at the N-terminal site of p53 is important for transcription and stabilization [12,13], but the dephosphorylation of N-terminal site has not been well studied. Here, we revealed for the first time a relationship between N-terminal phospho-serine 15 residue of p53 and PP1, and that phospho-serine 15 temporarily promotes the stability of p53 protein. By *in vitro* dephosphorylation assay (Fig. 3), we showed that PP1 actually dephosphorylated phospho-serine 15 of p53. However, it is still unclear whether other phosphorylated sites of p53 are dephosphorylated by PP1.

In conclusion, we propose that in response to UVC treatment, p53 is phosphorylated by the serine 15 kinases and continuously dephosphorylated by PP1 but not by PP2A. This dephosphorylation requires the phosphatase ability of PP1. The PP1 regulator GADD34 interferes with the dephosphorylation of p53 and increases the phosphorylation at serine 15 of p53. These results support the speculation that GADD34 regulates p53 by modulating its phosphorylation levels.

Acknowledgements: This study was supported by the Fund from the Ministry of Education, Science, and Culture of Japan.

References

- [1] Canman, C.E. et al. (1998) *Science* 281, 1677–1679.
- [2] Lambert, P.F., Kashanchi, F., Radonovich, M.F., Shiekhattar, R. and Brady, J.N. (1998) *J. Biol. Chem.* 273, 33048–33053.
- [3] Chehab, N.H., Malikzay, A., Appel, M. and Halazonetis, T.D. (2000) *Genes Dev.* 14, 278–288.
- [4] Hirao, A. et al. (2000) *Science* 287, 1824–1827.
- [5] Taylor, W.R. and Stark, G.R. (2001) *Oncogene* 20, 1803–1815.
- [6] Chehab, N.H., Malikzay, A., Stavridi, E.S. and Halazonetis, T.D. (1999) *Proc. Natl. Acad. Sci. USA* 96, 13777–13782.
- [7] Scheidtmann, K.H., Mumby, M.C., Rundell, K. and Walter, G. (1991) *Mol. Cell. Biol.* 11, 1996–2003.
- [8] Fiscella, M. et al. (1997) *Proc. Natl. Acad. Sci. USA* 94, 6048–6053.
- [9] Zuo, Z., Dean, N.M. and Honkanen, R.E. (1998) *J. Biol. Chem.* 273, 12250–12258.
- [10] Li, L., Ljungman, M. and Dixon, J.E. (2000) *J. Biol. Chem.* 275, 2410–2414.
- [11] Takenaka, I., Morin, F., Seizinger, B.R. and Kley, N. (1995) *J. Biol. Chem.* 270, 5405–5411.
- [12] Turenne, G.A., Paul, P., Laflair, L. and Price, B.D. (2001) *Oncogene* 20, 5100–5110.
- [13] Dohoney, K.M., Guillem, C., Whiteford, C., Elbi, C., Lambert, P.F., Hager, G.L. and Brady, J.N. (2004) *Oncogene* 23, 49–57.
- [14] Cohen, P., Holmes, C.F. and Tsukitani, Y. (1990) *Trends Biochem. Sci.* 15, 98–102.
- [15] Yatsunami, J., Komori, A., Ohta, T., Suganuma, M. and Fujiki, H. (1993) *Cancer Res.* 53, 239–241.
- [16] Zhang, W., McClain, C., Gau, J.P., Guo, X.Y. and Deisseroth, A.B. (1994) *Cancer Res.* 54, 4448–4453.
- [17] Mateer, S.C., Fedorov, S.A. and Mumby, M.C. (1998) *J. Biol. Chem.* 273, 35339–35346.
- [18] Yagi, A. et al. (2003) *J. Cell. Biochem.* 90, 1242–1249.
- [19] Kojima, E. et al. (2003) *FASEB J.* 17, 1573–1575.
- [20] Bai, L. and Merchant, J.L. (2001) *Mol. Cell. Biol.* 21, 4670–4683.
- [21] Gupta, V., Ogawa, A.K., Du, X., Houk, K.N. and Armstrong, R.W. (1997) *J. Med. Chem.* 40, 3199–3206.
- [22] Novoa, I., Zeng, H., Harding, H.P. and Ron, D. (2001) *J. Cell. Biol.* 153, 1011–1022.
- [23] Novoa, I., Zhang, Y., Zeng, H., Jungreis, R., Harding, H.P. and Ron, D. (2003) *EMBO J.* 22, 1180–1187.

Toll-like receptor 4 is expressed with enteroviral replication in myocardium from patients with dilated cardiomyopathy

Mamoru Satoh, Motoyuki Nakamura, Tomonari Akatsu, Yudai Shimoda, Ikuo Segawa and Katsuhiko Hiramori

Second Department of Internal Medicine, Iwate Medical University School of Medicine, Iwate, Japan

Expressions of innate immune response proteins, most notably proinflammatory cytokines, against enteroviral (EV) infection have been documented in the heart of human dilated cardiomyopathy (DCM). Toll-like receptor 4 (TLR4) activates signaling pathways leading to the expression of proinflammatory cytokines implicated the etiology of DCM. We sought to determine whether EV replication activates TLR4-dependent immune response in myocardium obtained from patients with DCM. Endomyocardial biopsy tissues were obtained from 56 patients with DCM and 10 controls. Levels of plus- and minus-strand EV RNA and TLR4 mRNA were measured by real-time RT-PCR. Immunohistochemical analysis was performed to identify the cellular source of EV capsid protein VP1 and TLR4. Both plus- and minus-strand EV RNA were detected in 19 DCM patients (34%). Neither strand of EV RNA was detected in controls. TLR4 mRNA levels were higher in DCM patients than in controls ($P < 0.001$). A positive correlation was found between TLR4 levels and each strand type of EV RNA in EV RNA-positive patients (plus-strand vs TLR4: $r = 0.69$, $P < 0.001$; minus-strand vs TLR4: $r = 0.65$, $P = 0.002$). VP1/TLR4 double staining showed extensive colocalization of VP1 and TLR4 proteins in cytoplasm of cardiac myocytes in myocardium obtained from DCM patients. EV RNA-positive patients showed lower systolic function and larger ventricular volume compared with EV RNA-negative patients left ventricular ejection fraction (LVEF): $P = 0.002$; left ventricular end-systolic diameter (LVESD): $P = 0.004$). The DCM subgroup with high TLR4 levels showed lower LVEF and larger LVESD than the subgroup with TLR4 levels (both $P < 0.001$). This study suggests that myocardial expression of TLR4 associates with EV replication in human DCM. EV RNA and TLR4 mRNA levels may correlate with LV dysfunction in DCM. The expression of TLR4 against EV replication may be involved in the pathogenesis of DCM.

Laboratory Investigation (2004) 84, 173–181, advance online publication, 15 December 2003; doi:10.1038/labinvest.3700031

Keywords: cytokines; immunology; infection/inflammation; signal transduction; viral diseases

Enteroviral (EV) RNA has been detected in a proportion of patients with dilated cardiomyopathy (DCM).^{1,2} It has been demonstrated that the detection of EV RNA in myocardium of DCM patients is associated with adverse prognosis.³ In particular, the presence of minus-strand EV RNA indicates active viral replication, and plays a role in the development of myocardial injury in DCM.⁴ Our previous study has reported that myocardial expression levels of tumor necrosis factor- α (TNF- α) and EV RNA were increased in patients with DCM regardless of etiology of left ventricular (LV) dysfunction.^{5,6} It is likely that an immune response against viral

pathogens is important in the pathogenesis of DCM. However, the precise mechanism underlying tissue injury in virus-mediated cardiomyopathy is not clear.

A family of toll-like receptors (TLRs) has recently been identified as a key component of pathogen-associated molecular pattern recognition machinery.⁷ At least nine types of human TLRs have recently been identified.⁷ It has been shown that active TLR4 led to expression of nuclear factor- κ B (NF- κ B)-controlled genes for proinflammatory cytokines that are required for activation of the immune response.⁸ TLR4 may therefore be an important factor in the signaling pathway in the host immune system in response to infectious disease. It has recently been reported that activation of antiviral immune response via TLR4 is important in the pathogenesis of viral infection.⁹

The purpose of this study was to determine whether TLR4 was expressed with EV replication,

Correspondence: M Satoh, Second Department of Internal Medicine, Iwate Medical University School of Medicine, Uchi-maru 19-1, Morioka 020-8505, Iwate, Japan.

E-mail: m_satoh@imu.ncvc.go.jp

Received 11 July 2003; revised 14 October 2003; accepted 17 October 2003; published online 15 December 2003

and to analyze the relationship between levels of TLR4 expression and clinical severity of DCM.

Materials and methods

Subjects

Endomyocardial tissues were obtained from 56 patients with primary DCM by right ventricular endomyocardial biopsy (42 male and 14 female patients; mean age 50.3 ± 2.2 years). The clinical diagnosis of DCM was made according to the World Health Organization/International Society and Federation of Cardiology Task Force criteria.¹⁰ Echocardiography was used to determine left ventricular ejection fraction (LVEF) and diameter immediately before the biopsy.

Control myocardial tissue samples were obtained by endomyocardial biopsy from 10 subjects (seven male and three female subjects; mean age 44 ± 12 years) with suspected cardiac disorder on the basis of ECG abnormality and echocardiographic changes, such as a slight increase in wall thickness without LV dysfunction. The resulting pathology findings showed no evidence of myocardial disease and these subjects were designated as controls. This study protocol was approved by our hospital ethics committee, and written informed consent was obtained from all subjects.

As a positive control of RT-PCR for EV RNA detection, we used HeLa cells incubated with 10^6 plaque-forming units coxsackievirus B3 (CVB3) (Nancy strain).

Extraction of RNA

Total RNA was extracted from endomyocardial tissues and positive control cells by the acid guanidinium thiocyanate-phenol-chloroform method, and treated with DNase I (GIBCO BRL).¹¹

Primers and TaqMan Probes

Plus- and minus-strand EV RNAs were amplified by using two sets of primers and TaqMan probes that recognized the 5' uncoding genomic region (forward primer: 5' GGG CGC TAG CAC TCT GGT AT 3', reverse primer: 5' GCC GGA TAA CGA ACG CTT T 3' and TaqMan probe: 5' ATC AAG CAC TTC TGT TAC CCC GGA CTG A 3').¹² The published sequence for human TLR4 was used for construction of primers and TaqMan probe (forward primer: 5' TGA TTG TTG TGG TGT CCC A 3', reverse primer: 5' TGT CCT CCC ACT CCA GGT AA 3' and TaqMan probe: 5' TCC TGC AGA AGG TGG AGA AGA CCC T 3').⁸ For all myocardial specimens, glyceraldehyde-3-phosphate dehydrogenase (GAPDH) mRNA was amplified using TaqMan GAPDH control reagents as an internal control (PE Biosystem, Foster City, CA, USA).

Real-time RT-PCR

Total RNA of each biopsy was transcribed into cDNA of TLR4 and GAPDH by MultiScribe RT with random hexamers (TaqMan Gold RT-PCR kit, PE Biosystem). In separate experiments to determine the polarity of EV RNA, the cDNA of plus-strand EV RNA was synthesized in $10 \mu\text{l}$ of solution containing 100 ng total RNA, $10 \times$ TaqMan RT-buffer, 10 mM deoxyNTPs mixture, 20 mM EV reverse primer and 1.25 IU MultiScribe RT as described by the manufacturer. The cDNA of minus-strand EV RNA was synthesized in the same way using EV forward primer instead of EV reverse primer. The RT reaction was performed at 37°C for 30 min, and heated at 95°C for 5 min to inactivate RT activity.

PCR mixture was added to each RT mixture containing 0.025 U AmpliTaq Gold DNA polymerase, AmpErase UNG, 25 mM MgCl_2 , primer and TaqMan probe, and $10 \times$ TaqMan buffer A. Each of 40 reaction cycles consisted of denaturation for 15 s at 95°C , and annealing and extension for 1 min at 60°C . To improve the accuracy of real-time RT-PCR for quantification, amplifications were performed in triplicate for each RNA sample. To account for variations in input RNA and RT efficiency, EV RNA and TLR4 levels were normalized to GAPDH expression in each sample. To account for PCR amplification of contaminating genomic DNA, a control without RT was included.

Immunohistochemistry

EV capsid protein VP1/TLR4 double staining was performed on serial paraffin sections to determine the cellular source of EV capsid protein VP1 and TLR4. Monoclonal mouse anti-enterovirus against EV capsid protein VP1 (Dako, Glostrup, Denmark) and mouse monoclonal IgG_{2a} against human TLR4 (Santa Cruz Biotechnology) were used as primary antibodies. The tissue sections were deparaffined and thoroughly dehydrated. After inhibition of endogenous peroxidase and blocking of non specific reactions, mouse monoclonal IgG_{2a} against human TLR4 was applied. Biotinylated mouse immunoglobulin was used as a secondary antibody. Peroxidase-labeled streptavidin (Histofine, MAX-PO kit, Nichiren Corp) was applied and visualized using diaminobenzidine as a chromogen.

For double-staining, mouse monoclonal IgG_{2a} against human TLR4 was first stained as mentioned above. Thereafter, the sections were incubated with monoclonal mouse anti-enterovirus against EV capsid protein VP1 at 4°C overnight, followed by incubation for 30 min with rabbit anti-mouse immunoglobulin and alkaline phosphatase anti-alkaline phosphatase, and visualized with FastBlue (Histofine, SAP-AP kit, Nichiren Corp). The specificity of the immunohistochemistry was confirmed by substituting the primary antibodies with mouse

IgG1 negative control (Dako) on control sections from patients with DCM.

Statistical Analysis

All values are presented as mean \pm s.e. Statistically, the differences in EV RNA and TLR4 expression levels between the DCM and control groups were analyzed by unpaired *t* test. Pearson's correlation coefficients were used to examine the relationship between levels of mRNA expression and clinical parameters. A value of $P < 0.05$ was considered statistically significant.

Results

EV RNA and TLR4 mRNA Levels in Myocardial Tissues

Plus- and minus-strand EV RNAs were detected in 19 (34%) of the 56 patients with DCM (mean levels of plus-strand EV RNA/GAPDH ratio and minus-strand EV RNA/GAPDH ratio in EV RNA-positive patients with DCM: 1.63 ± 0.37 and 1.27 ± 0.30 , respectively). All patients who were positive for minus-strand EV RNA were also positive for plus-strand EV RNA. A positive correlation was found between plus- and minus-strand EV RNA levels in EV RNA-positive patients with DCM ($r = 0.90$, $P < 0.001$) (Figure 1). Neither strand of EV RNA was detected in controls. In infected HeLa cells, the level of plus-strand EV RNA was higher than that of minus-strand EV RNA (plus-strand EV RNA/GAPDH ratio: 24076.68 ± 1830.32 , minus-strand EV RNA/GAPDH ratio: 285.61 ± 14.15).

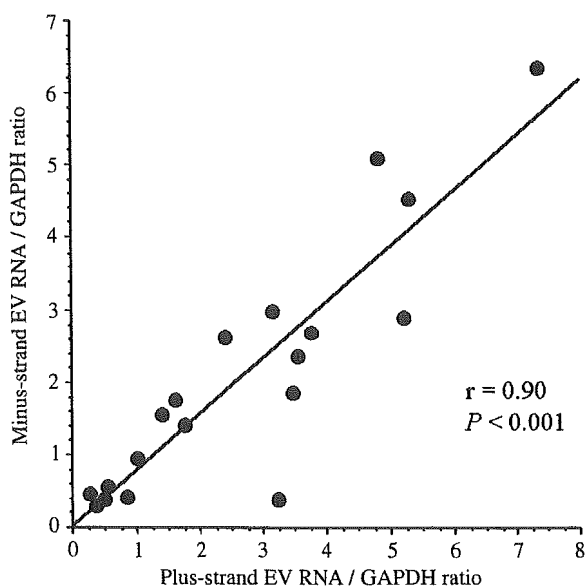


Figure 1 Correlation plot between plus- and minus-strand EV RNA levels in myocardium obtained from patients with DCM. Significant correlation: $r = 0.90$, $P < 0.001$.

TLR4 mRNA levels were higher in patients with DCM than in controls (TLR4/GAPDH ratio: 0.24 ± 0.03 vs 0.01 ± 0.004 , $P < 0.001$). TLR4 mRNA levels were higher in EV RNA-positive DCM patients than in EV RNA-negative DCM patients (TLR4/GAPDH ratio: 0.38 ± 0.06 vs 0.16 ± 0.03 , $P = 0.001$) (Figure 2). A weak positive correlation was found between each strand of EV RNA and TLR4 mRNA levels in 19 EV RNA-positive patients with DCM (plus-strand EV RNA vs TLR4: $r = 0.69$, $P < 0.001$; minus-strand EV RNA vs TLR4: $r = 0.65$, $P = 0.002$).

Immunohistochemistry for TLR4 and EV Capsid Protein VP1

EV capsid protein VP1 was detected in 17 of the 56 patients with DCM (30.3%). As shown in Figure 3a, immunostaining of VP1 was observed in cytoplasm of cardiac myocytes in myocardium from patients with DCM. VP1 signals were found in scattered cardiac myocytes and myofibers in DCM. Both plus- and minus-strand EV RNA were detected in all VP1-positive patients with DCM. TLR4 immunostaining was positive in 35 patients with DCM (62.5%). VP1/TLR4 double staining showed extensive colocalization of VP1 and TLR4 proteins in cytoplasm of cardiac myocytes in myocardium obtained from DCM patients (Figure 3a). TLR4 mRNA levels were

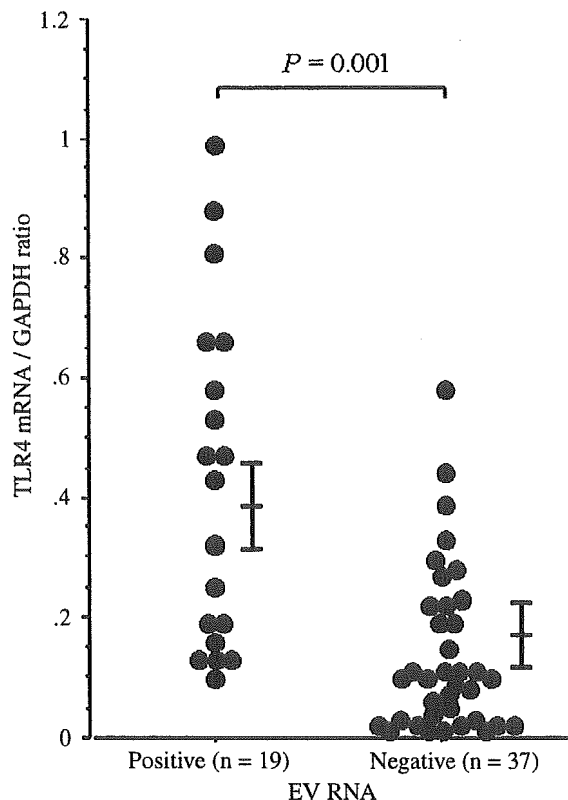


Figure 2 Comparison of TLR4 mRNA levels between EV RNA-positive DCM patients and negative DCM patients.